DOI 10.1007/s10946-022-10056-z
Journal of Russian Laser Research, Volume 43, Number 3, May, 2022

GENERATION OF A 294.2 nm ULTRAVIOLET BEAM THROUGH FREQUENCY DOUBLING IN A BaB_2O_4 CRYSTAL

Ji Yao,[1,2] Quan Zheng,[1,3*] Yuning Wang,[3] Qi Li,[3] and Wei Huang[1]

[1] *Changchun Institute of Optics, Fine Mechanics and Physics Chinese Academy of Sciences Changchun, Jilin 130033, China*

[2] *University of Chinese Academy of Sciences Beijing 100190, China*

[3] *Changchun New Industries Optoelectronics Tech. Co. Ltd. Changchun 130012, China*

*Corresponding author e-mail: zhengquan@cnilaser.com

Abstract

We demonstrate a 294.2 nm all-solid-state Q-switched laser, with 241.4 mW average output power, produced by frequency doubling of a 588.4 nm laser. The 588.4 nm laser is obtained by intracavity sum-frequency generation of a 1064 nm laser and a 1319 nm laser. By synchronizing the fundamental lasers and adjusting the focal length of the focusing lens, average output powers of 10.2 W at 588.4 nm and 241.4 mW at 294.2 nm with 297 ns pulse width are obtained at 6 kHz frequency. The 294.2 nm laser beam quality $M_X^2 = 1.18$ and $M_Y^2 = 1.26$ for the X and Y directions, respectively. To the best of our knowledge, this is the highest power of all-solid-state Q-switched laser at 294.2 nm.

Keywords: Q-switched laser, ultraviolet laser, nanosecond laser.

1. Introduction

Ultraviolet (UV) lasers have promising applications in spectroscopy, environmental sensing, chemical detection, and industry [1–6]. Also they have advantages with regard to lifetimes, maintenance costs, system volume, and work efficiency. Specifically, continuous-wave (CW) 294 nm lasers have been used for cooling and collimating gallium atoms because the wavelength is resonant with the $4p^2P_{3/2} \rightarrow 5d^2D_{5/2}$ gallium transition [7–9]. Nanosecond-pulsed 294 nm lasers are mainly used in industrial processing because of the high peak powers and detection sensitivity; nevertheless, only few reports have been published and the beam quality has not been discussed [10–12]. Here, a 241.4 mW, Q-switched 294.2 nm laser with a 297 ns pulse width is obtained by frequency doubling of a 588.4 nm laser with a β-BaB_2O_4 (BBO) crystal. The 588.4 nm laser is obtained by sum-frequency generation of a 1064 nm and a 1319-nm fundamental lasers. We use a cylindrical lens to shape the 294.2 nm laser beam, and the beam quality $M_X^2 = 1.18$ and $M_Y^2 = 1.26$ for the X and Y directions, respectively.

Manuscript submitted by the authors in English on August 27, 2021.

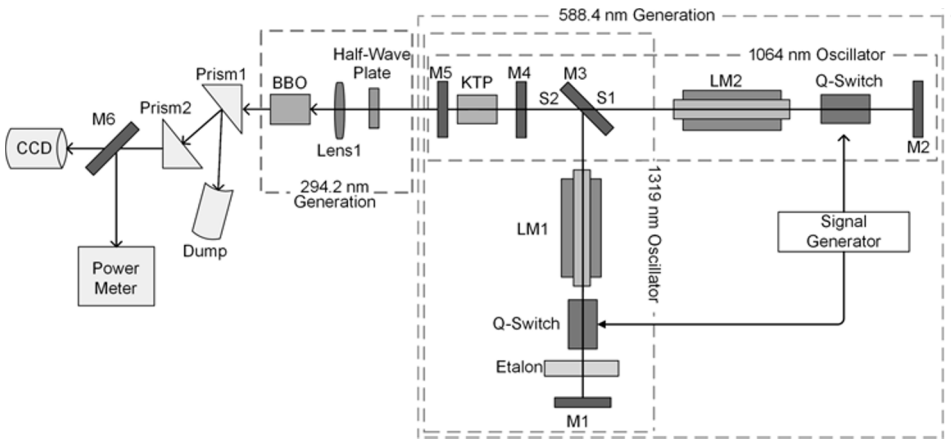

Fig. 1. Schematic of Q-switched 294.2 nm laser. Here, M1 is a 1319 nm high-reflection (HR)-coated mirror, M2 is a 1064 nm HR-coated mirror, M3 is a beam splitter, M4 is antireflection (AR)-coated at 1319 nm and 1064 nm (of fundamental lasers) and HR-coated at 588.4 nm, and M5 is an output mirror with HR-coating for fundamental lasers and AR-coating at 588.4 nm.

2. Experimental Setup

A schematic of Q-switched 294.2 nm laser is shown in Fig. 1. The overall optical layout comprises a 1064 nm oscillator, a 1319 nm oscillator, a 588.4 nm laser generator, and a 294.2 nm laser generator.

The 1064 nm oscillator consists of HR-coated mirror M2, a 1064 nm acousto-optic Q-switch (the aperture of optical elements $\varnothing 3\times 30$ mm) that provides the generation of nanosecond pulses, a high-power diode-side-pumped laser module (LM2), beam splitter M3, fundamental lasers, AR-coated and 588.4 nm HR-coated mirror M4, and output mirror M5. The laser module (LM2) has a Nd:YAG rod gain medium ($\varnothing 3\times 70$ mm) doped with 1% Nd^{3+}, with the end face being AR-coated at 1064 nm. The gain rod is three-fold symmetrically side-pumped at 808 nm with three 40 W laser-diode arrays.

The 1319 nm oscillator is composed of HR-coated mirror M1, an etalon of 1319 nm laser which is used to narrow the line width, a 1319 nm acousto-optic Q-switch ($\varnothing 3\times 30$ mm), LM1 with the same structure as that for the 1064 nm oscillator, except different coatings, beam splitter M3, fundamental lasers, AR-coated and 588.4 nm HR-coated mirror M4, and output mirror M5. As shown in Fig. 1, the M3, M4, and M5 are common components of the two oscillators; thus, they make up the co-folding arm.

The polarization beam splitter M3 is used to generate p-polarized 1064-nm laser beam and s-polarized 1319 nm laser beam due to corresponding different coating of the two surfaces. The surface S1 of polarization beam splitter M3 is coated with 45° p-polarized antireflection and s-polarized high-reflection at 1064 nm. The surface S2 of polarization beam splitter M3 is coated with 45° antireflection at 1064 nm, and 45° p-polarized antireflection and s-polarized high-reflection at 1319 nm. As a result, the polarization beam splitter M3 provides the p-polarized 1064 nm laser and the s-polarized 1319 nm laser.

The 588.4 nm intracavity sum-frequency generation system involves mirror M4, a potassium titanyl phosphate (KTP) crystal [13], the output mirror M5, and a signal generator used to control the frequency and delay of fundamental lasers. The M4 is AR-coated for fundamental lasers and HR-coated at 588.4 nm; it is used to reflect the 588.4 nm sum-frequency generation of the fundamental lasers. Finally, M5 is a 588.4 nm output mirror.

The 294 nm generation system involves a half-wave plate at 588.4 nm, a focusing lens at 588.4 nm, and a BBO crystal ($\varnothing 2\times 10$ mm and the cutting angle of nonlinear crystal $\theta = 41.7°$). The half-wave plate is used for rotating the 588.4 nm polarization direction to a horizontal orientation, and lens 1 is used to focus the 588.4 nm laser in the BBO crystal to improve the peak-power density and the frequency-

doubling efficiency. The BBO crystal is used because it has a large nonlinear coefficient; it is produced from a mature-growth technology [14].

Prisms 1 and 2 are used to separate the 588.4 nm laser and 294.2 nm laser, and a cylindrical lens is used for shaping the beam profile of the 294.2 nm laser. The 45° HR-coated mirror M6 at 294.2 nm is used to measure the 294.2 nm power and the beam quality.

3. Experimental Results and Discussion

Because of different gains and threshold powers of the 1064 nm laser and 1319 nm laser, the timing of the outputs is different, as shown in Fig. 2 a. Hence, a pulsed electronic synchronizer was used to synchronize the fundamental lasers. First, we measured the pulse profiles with photodetector and digital oscilloscope, then compensated the difference time by adjusting the delay time of a signal generator, providing in such a way the control of the repetition rate and triggering of the corresponding Q-switches. As shown in Fig. 2 b, the pulse profiles of fundamental lasers entirely overlap with a 550 ns delay time, and the 588.4 nm average power is up to a maximum of 10.2 W.

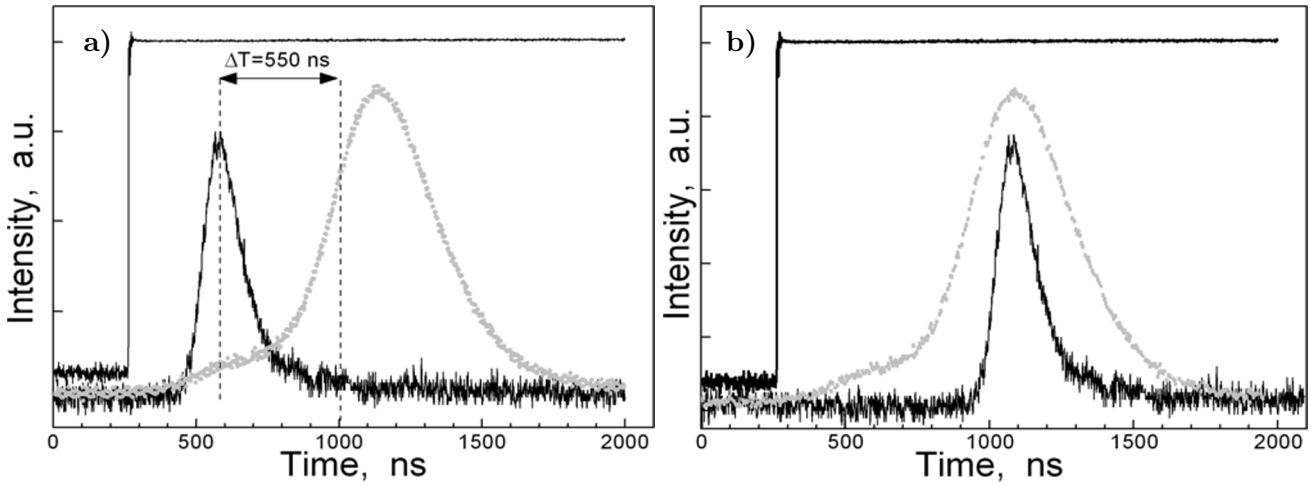

Fig. 2. Pulse profiles of fundamental lasers without an electronic delay (a) and with a 550 ns electronic delay (b). Here, the reference signal (the topmost black curve), signal at 1319 nm (the dotted gray curve), and signal at 1064 nm (the bottom solid curve).

The 588.4 nm spectrum is shown in Fig. 3. The average output power curves of the 294.2 nm laser with different focal-lengths are shown in Fig. 4 a, where F is the focal length of Lens 1. The frequency-doubling efficiency and the output power increase with reduced focal lengths and increased 588.4 nm power. With 10.2 W of the 588.4 nm laser focused into the BBO crystal with a 15 mm focal-length lens, mean power of 241.4 mW with standard deviation of 6 mW at 294.2 nm is obtained at a 6 kHz repetition rate. The second-harmonic con-

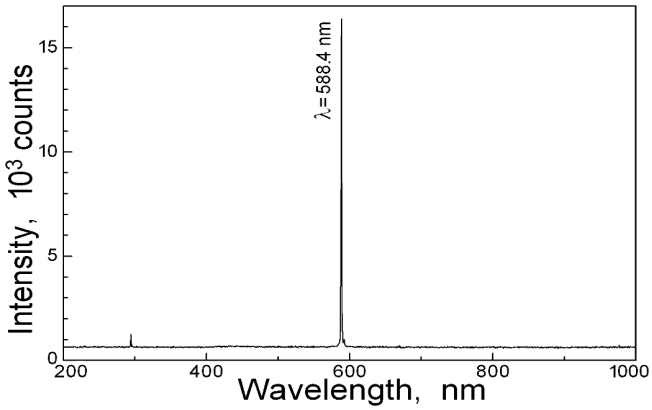

Fig. 3. Spectrum of the 588.4 nm laser.

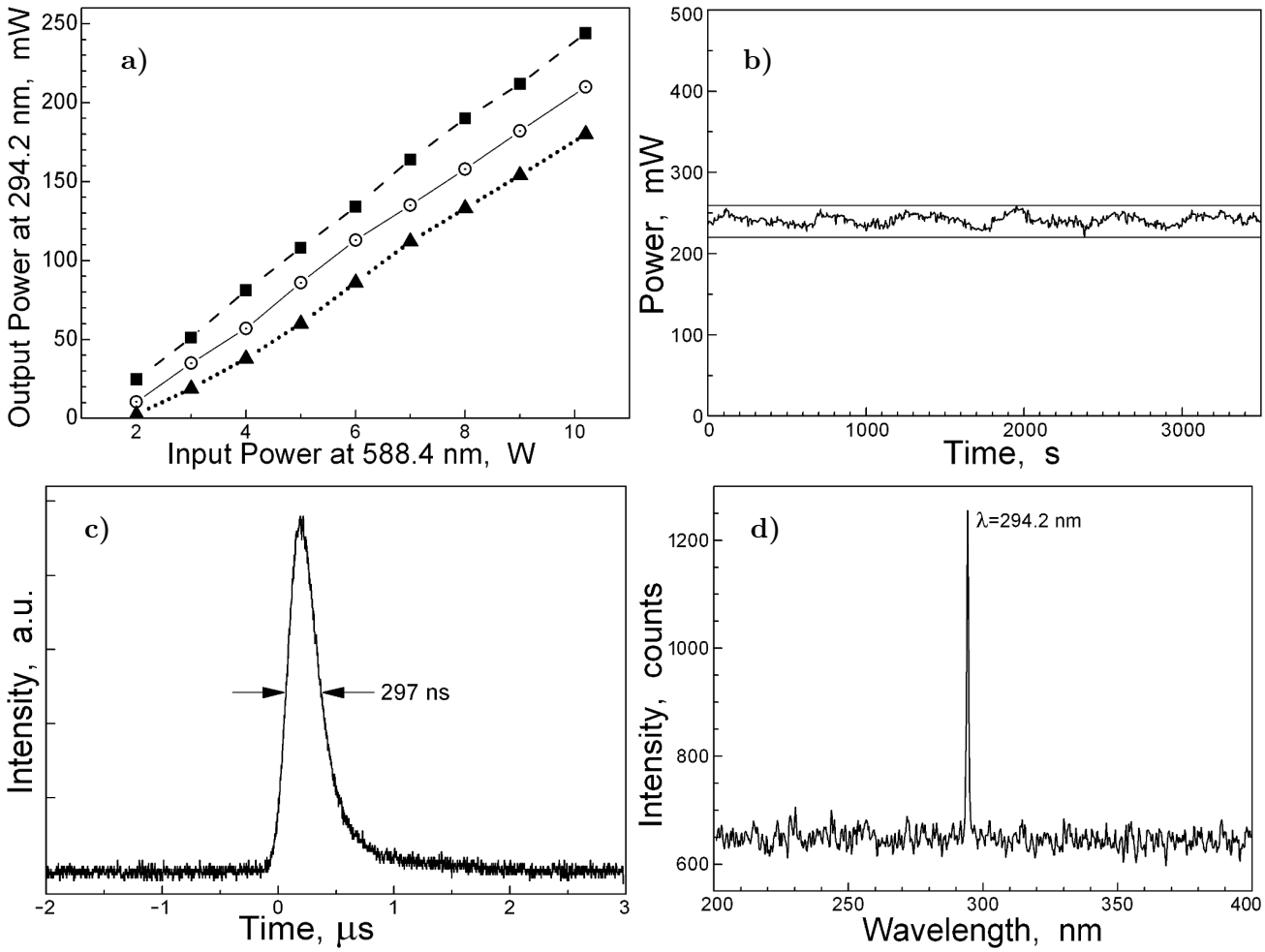

Fig. 4. Variation of 294.2 nm output power for different focal length F of Lens 1 used for frequency doubling (a), in time (b), the power stability (c), and the pulse profile spectrum of the 294.2 nm laser (d). Here, $F = 15$ mm (■), $F = 22$ mm (⊙), and $F = 30$ mm (▲).

version efficiency is close to 2.4%, and there are three reasons for the low conversion efficiency. The first reason is a low nonlinear coefficient of frequency doubling and small peak power density of the 588.4 nm laser. The second reason is the fact that the BBO crystal has a large horizontal walk-off effect at the 588.4 nm frequency doubling, and this leads to decrease of the second-harmonic conversion efficiency. Finally, the phase mismatching appears due to excessive incident angle.

As shown in Fig. 4 a, we use a 15 mm focal-length lens to increase the output power because the smaller the focal spot, the higher the peak power density we can get. But with the focal length decrease, the incident angle increases and gets bigger than the acceptance angle in the X direction, and this fact leads to the angle phase mismatching, providing decrease of the second harmonics conversion efficiency. The angle phase mismatching is the main reason of the low conversion efficiency. As shown in Fig. 4 b, the average power is 241.4 mW with a standard deviation of 5.98 mW over 1 h. The pulse profile and spectrum of the 588.4 nm laser is shown in Fig. 4 c and d.

Since the BBO crystal has a large horizontal walk-off effect in frequency doubling, the horizontal dimension of the 294.2 nm laser is much longer than the vertical dimension. A 40 mm focal-length cylindrical lens is used to symmetrically shape the beam, and the beam quality of the 294.2 nm laser after shaping is shown in Fig. 5. The beam quality is $M_X^2 = 1.18$ and $M_Y^2 = 1.26$ for the X and Y directions, respectively.

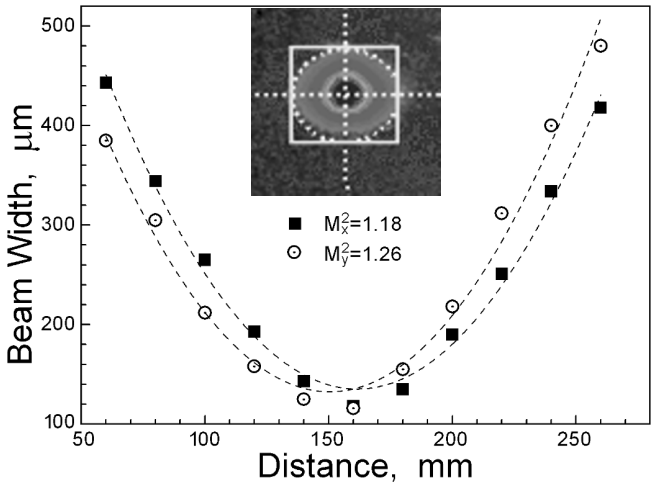

Fig. 5. The beam quality of the 294.2 nm laser. X direction is shown by ■ and Y direction – by ⊙.

4. Conclusions

In summary, we developed an all-solid-state Q-switched 294.2 nm laser designed through external-cavity frequency doubling in a BBO crystal, in view of the intracavity sum-frequency generation of a 588.4 nm laser in an KTP crystal. An average power of the 294.2 nm laser is 241.4 mW at 6 kHz with a pulse width of 297 ns and beam quality $M_X^2 = 1.18$ and $M_Y^2 = 1.26$. In the future, we plan to improve the conversion efficiency and output power of the 294.2 nm laser by optimizing the structure of laser cavities.

References

1. A. N. Kuryak and B. A. Tikhomirov, *Quantum Electron.*, **50**, 876 (2020).
2. M. Rui, L. Pereira, T. Paixao, et al., *Opt. Express*, **27**, 38039 (2019).
3. B. Behera and P. Das, *Chem. Phys. Lett.*, **774**, 138601 (2021).
4. S. J. Park, J. H. Song, and G. A. Lee, *Adv. Mat. Res.*, **490**, 238 (2012).
5. L. R. Kong, F. Zhang, J. Duan, et al., *Laser Technol.*, **38**, 330 (2014).
6. S. D. Alaruri, *Optik*, **181**, 239 (2019).
7. C. D. Marshall, J. A. Speth, S. A. Payne, et al., *J. Opt. Soc. Am. B*, **11**, 2054 (1994)
8. M. A. Dubinskii, K. L. Schepler, R. Y. Abdulsabirov, and S. L. Korableva, "Tunable UV Ce:LiCAF Injection-Seeded Laser for High Spectral Brightness Applications," *Advanced Solid State Lasers Conference*, Optical Society of America, Coeur d'Alene (1998); DOI: 10.1364/ASSL.1998.UL2
9. M. Fallahi, L. Fan, Y. Kaneda, et al., *IEEE Photon. Technol. Lett.*, **20**, 1700 (2008).
10. Y. Kaneda, M. Fallahi, J. Hader, et al., *Opt. Lett.*, **34**, 3511 (2009).
11. G. P. Lin and N. Yu, *Opt. Express*, **22**, 557 (2014).
12. M. A. Khan, N. Maeda, M. Jo, et al., *J. Mat. Chem. C*, **7**, 143 (2018).
13. Y. Liu, Z. J. Liu, Z. H. Cong, et al., *Opt. Laser Technol.*, **81**, 184 (2016).
14. K. S. Chaitanya, C. J. Canals, B. E. Sanchez, et al., *Opt. Lett.*, **40**, 2397 (2015).